Fatigue strength of CFRP strengthened welded joints with corrugated steel plates

Zhi-Yu Wang *, Qing-Yuan Wang

Department of Civil Engineering & Mechanics, Institute of Architecture and Environment, Sichuan University, Chengdu, PR China
Key Laboratory of Energy Engineering Safety and Disaster Mechanics, Ministry of Education, Sichuan University, Chengdu, PR China

This paper presents an experimental and numerical research on the carbon fibre reinforced polymer (CFRP) strengthened welded joints with corrugated plates. The effectiveness of the strengthening in the improvement of fatigue strength has been examined experimentally on the test joints through varying the number and the layout of the CFRP laminates. The test results show that the joints with transition curvature region reinforcement and single side reinforcement produce slightly lower rigidity but longer fatigue life in contrast to those with full width reinforcement on the double side of the main plate. Fur-thermore, a simplified two dimensional analytical model which allows for the geometric characteristics of the joint has been proposed to investigate the stress intensity factor of mode I. The proposed analytical model has been simulated by finite element technique and its solution result is compared with previously reported theoretical calculation. Parametric studies have been performed to investigate the effects of the number of CFRP layers and the moduli of carbon fibre & adhesive on the stress intensity factor. The com-bined influence of the corrugation angle and crack depth has also been considered. It has been found that these effects on the stress intensity factor are more significant for the joints with smaller corrugation angle.

Keywords:
A. Carbon fibre
B. Fatigue
B. Stress concentrations
E. Joints
Corrugated plate

1. Introduction

Fatigue damage cases in steel bridges have raised growing concern in recent years [1,2]. Fatigue is usually the cause for the cracks identified at bridge elements in service [3]. The propagation of an unmitigated crack will trigger a fracture of a structural member which may further lead to partial or total structural deficiency of the bridge. Moreover, the fatigue deterioration process is affected by various factors, such as aggressive environmental condition, deterioration of materials, heavy traffic load beyond old design restriction and insufficient maintenance. This fact thus generates an increasing need for effective means of structural retrofit of steel bridges.

Among several methods for upgrading structural members, the use of carbon fibre reinforced polymer (CFRP) and glass fibre reinforced polymers (GFRP) to adhesively bond the damaged member for the sake of increasing the loading-carrying capacity has received excellent application in the civil and mechanical engineering fields [4–8]. Apart from flexible shapes and high strength to weight ratios, the merits of having good constructability and durability of non-metallic CFRP composites also make them quite promising for the strengthening of steel structures [11]. Fundamental research projects and experimental investigations [9–16] have examined the effectiveness of using CFRP technology in bettering the fatigue behaviour of steel girders and frame connections. As a countermeasure to the fatigue cracks at the typical weld-assembled location in bridge structures [2], recent examinations have also been conducted to evaluate the validity of the fibre reinforced polymer (FRP) retrofitting in typical welded details of steel bridges. In contrast to the researches focused on the steel structural elements, however, this part of study is limited. Inaba et al. [17] conducted fatigue tests on the cruciform welded joints patched with GFRP composites. Their tests showed the stress concentration at local weld toe can be improved to some extent as a result of GFRP repair. Nakamura et al. [18] studied CFRP retrofitted welded web gusset joints under fatigue loading. By comparing several repair methods, they gave a practical method of using CFRP in extending fatigue life of such joints. Chen et al. [19] performed several fatigue tests by repairing with CFRP on the cruciform welded joints. The results computed by local stress approach showed better fatigue performance with CFRP sheets. Besides, finite element

* Corresponding author.
E-mail address: zywang@scu.edu.cn (Z.-Y. Wang).

Published Journal Article available at: http://dx.doi.org/10.1016/j.compositesb.2014.11.021

analysis was also employed in several reported studies [18,20] to investigate the stress characteristics and stress intensity factor at the common welded joints mentioned above.

The use of corrugated web to enhance the web's out-of-plane stiffness and buckling resistance as a substitute to the involvement of stiffeners or thicker webs has been recognized in the field of structural engineering. Since 1980s, the corrugated steel webs in I or box section girders have been employed in a number of highway bridge constructions in Europe and Asia [21,22]. Recently, their long-term structural response and life improvement under repeated loads have been paid increasing attention. The corrugated steel web girders often failed from fatigue cracks that propagated from the web-to-flange fillet weld toe on the tension flange [23]. The stress distribution of such welded details differs considerably from that of common welded joints reported formerly, especially due to the variation of the corrugation on the flange plate. It therefore seems insufficient to directly import formerly reported repair methods in common welded joints for the reinforcement of such welded details subjected to fatigue loading.

Regarding the structural fatigue behaviour, the experimental work conducted previously by the authors has demonstrated a good applicability of a specific weld joint with the corrugated plate in the representation of the welded details in the corrugated steel web girders [24,25]. As a follow-up study, the aim of this work was to investigate such welded details strengthened with CFRP and to gain a first experience with related life extension using different CFRP composites and joint geometric characteristics. This paper will present the fatigue experimental results of repair effects with varying number and layout of CFRP sheets or strips for the mitigation of fatigue failure on the tension flange of the corrugated steel web girder without the introduction of local buckling and compression. The fatigue life of the studied joints after reinforcement is compared with typical welded details codified in the AASHTO LRFD [26]. Afterwards, an analytical model taking into account the corrugation angle with the configuration of the welds is reported. The model has been developed with the aid of finite ele-ment simulation technique to study the stress intensity factor of mode I of such joints. Through a parametric study, the effects such as the number of CFRP layers and the elastic moduli of carbon fibre & adhesive on the reinforcement under the variation of crack length and corrugation angle are also indicated.

2. Experimental details

2.1. Strengthening scheme

The test results of previous study indicated that the welded details in the vicinity of the transition curvature between the longitudinal fold and the inclined fold of the corrugated plate are susceptible to suffer fatigue cracking. Regarding this, four CFRP strengthening methods were adopted for the rehabilitation of such locations of the welded joints in the experimental work. The illustration of CFRP sheet and strip arrangement is shown in Table 1.

In the welded joint series D-S-F, single-layered CFRP sheets were bonded to both sides of the weld bead close to the transition curvature as well as the bottom surface of the main plate of full width in order to reduce the stress concentration at crack tips. This is taken as a basic reference for the comparison with following arrangements, as illustrated in Table 1(i). The welded joint series D-T-F was strengthened using three-layered CFRP sheets attachment and the welded joint series S-S-F was reinforced with single-layered CFRP sheets only on the one side of the main plate containing welded details. Additionally, the CFRP strips instead of sheets were used to cover only the transition curvature location correspondingly on the both sides of the main plate in the welded joint series D-S-T, as illustrated in Table 1(ii).

The application of CFRP sheets or strips on the welded joints was started by grinding the surface of the joint to remove rust until the metal surface was exposed over the area for strengthening. Afterwards, the surface was abraded and wiped with cotton cloth soaked in acetone. The CFRP sheets or strips were then applied over the joint surface preceded by spreading adhesive according to the strengthening arrangement mentioned above. When CFRP sheets or strips were applied, the pressure was gently imposed on the laminate surface to ensure proper and even bond condition.

2.2. Details of specimens and materials

The basic geometry of the test specimen is shown in Fig. 1. It was fabricated with corrugated steel plate, containing the longitudinal fold & the inclined fold and the transition curvature, welded to the one side of the main plate. Based on the work previously done by the authors, two characteristic parameters are referred as: θ_c which is defined as the corrugation angle of the inclined fold to the stress in longitudinal direction and γ which is defined as the ratio of the curvature radius to the depth of the corrugation, as also illustrated in Table 1. θ_c and γ were taken as 60°and 0.75 respectively for the welded joints tested in this study. The steel plates used for the test specimens are 6 mm and 3 mm thick for the main plate and the corrugated plate respectively. The carbon fibre in the longitudinal direction was arranged to cover the full length of the longitudinal fold & the inclined fold and the transition curvature, representative of a half-unit of the corrugation. Apart from covering the full width of the main plate using CFRP sheets in the welded joint series D-S-F, D-T-F and S-S-F, the CFRP strips were also adopted in the welded joint series D-S-T strengthening only the transition curvature part.

The steel used for all specimens conforms to Q345 steel of the Chinese national standard GB/T 1591-2008 [27]. High performance carbon fibre sheet UT70-30 with the thickness of 0.167 mm produced by Toray Industries, Inc, and adhesive Araldite XH 180 manufactured by Huntsman Advanced Materials Co. Ltd were adopted for the application of CFRP sheets & strips on the steel plates. Related mechanical properties and chemical composition are described in Table 2. The design weld leg length (a_f) is 3 mm for all fillet welds. CO_2 shielded semiautomatic Gas Metal Arc Welding (GMAW) was performed for all fillet welds joining the main plates and the corrugated plates. The welding stop-starts were avoided during welding process.

2.3. Test setup and procedure

The fatigue tests were performed through a MTS 809 servo-hydraulic fatigue testing machine with 100 kN capacity. As shown in Fig. 2, the one end of the main plate of the welded joint was gripped in the bottom head of the test machine with special clamp splices to ensure that only the main plate is involved with directly applied longitudinal tensile stress. Meanwhile, the other end of the main plate was gripped in the fixed upper head of the test machine to provide reaction load. In this way, the fillet weld is not carrying the appreciable part of the tensile load but strained by the load in its joined stressed main plate. Output and instant information from the testing machine were monitored and recorded by an automatic data acquisition system controlled by MTS Series 793 software. Constant amplitude sinusoidal stress cycles with the frequency of 8 Hz were conducted during the fatigue test. The target stress range levels between 135 MPa and 200 MPa were chosen and the stress ratio was set at 0.1 for all tests. The fatigue life was deter-mined as the test specimen was tested to rupture. The actual mea-sured cross-sectional dimensions were used for the calculation of nominal stress of testing specimens. For strain measurement and

Table 1
Application of CFRP onto the welded joints with corrugated steel plates.

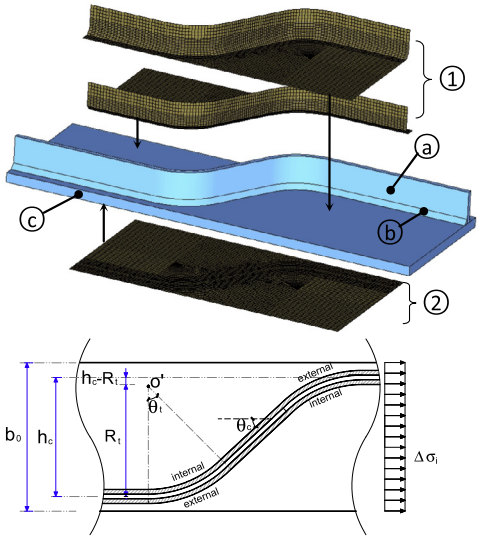

θ_c-corrugation angle of the inclined fold to the stress in longitudinal direction;

γ-the ratio of the curvature radius (R_t) to the depth of corrugation (h_c)

Ref.	CFRP strengthening pattern		
	①	②	Illustration graph
D-S-F	1 layer	1 layer	(i)
D-T-F	3 layers	3 layers	(i)
S-S-F	1 layer	N/A	(i)
D-S-T	1 layer*	1 layer*	(ii)

Note:
a. Corrugated plate
b. Fillet weld
c. Main plate (flange)
1. Adhesive CFRP layers (top)
2. Adhesive CFRP layers (bottom)

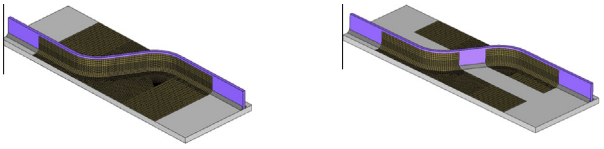

(i) (ii)

Graph (i) denotes the adhesion of CFRP sheets onto the full corrugation and its related main plate location.
*Graph (ii) denotes longitudinal CFRP strips are clipped only covering the transition curvature and parallel fold of the corrugated plate and its related main plate location.

rigidity comparison, a part of monotonic loading test was also conducted prior to the cyclic loading procedure.

3. Experimental results

3.1. Crack initiation and propagation modes

The fatigue crack growth regions were evaluated substantially dependent on the visual examination of the crack mode and its related fracture surface of the welded joints. Therefore, the strengthening effect of CFRP laminate on the welded joints was investigated in the test programme. For the purpose of post-test observation, local damaged CFRP laminates were trimmed using cutting tools. The examination of the fracture location displayed in Fig. 3 indicated that the typical fatigue failure of the welded joints occurred in the region of the transition curvature between the longitudinal fold and the inclined fold of the corrugated plate. On closer examination, the fracture surfaces are mostly located close to the vicinity of the end of the inclined fold joining transition curvature. During the fatigue loading process, four stages of fatigue crack life can be estimated as: (1) interface failure between steel and adhesive; (2) crack initiation at the weld toe of the external weld line; (3) crack penetration into the thickness of the main plate; (4) crack propagation in the width direction perpendicular to the applied tensile stress.

The fractured part of the welded joint was further used to examine and verify aforementioned cracking modes. Fig. 4 shows typical fatigue fracture surfaces along with crack growth striations of approximately 30 magnifications under the scanning electron microscope (SEM) for the test welded joints with different strengthening scheme. The crack can be seen to originate at the weld toe and propagate into the main plate (stage 2). The presence of fatigue striations verified the further development of fatigue cracks through the thickness of the main plate (stage 3). The crack propagation pattern on the fracture surface can be idealized as a semi-elliptical shape. Near the edge of the main plate the crack path moved away from the weld toe and tensile fracture occurred locally as evidenced by some discernible necking (stage 4).

Referring to Fig. 3 again, the inspection indicates that the cause of fatigue cracking was the stress concentration at the transition curvature between the longitudinal fold and the inclined fold of the corrugation and its related welded toe line. Fatigue crack growth striations are also apparent near the crack initiation points. Based on the examination, the influence of different CFRP strength-ening methods on the fatigue crack propagation modes can be identified as follows.

The specimen series D-S-F (Fig. 4a) and D-T-F (Fig. 4b) which are reinforced by single and triple CFRP sheets show similar crack growth pattern on the fracture surface. The crack initiation location of the series D-T-F is slightly further away from the edge of the plate when compared with that of the series D-S-F. For the specimen series S-S-F (Fig. 4c), the length of major axis of the semi-elliptical pattern is somewhat reduced on the fracture surface. This can be attributed to the change of the local stress distribution along the crack path as only the one side with fillet weld is strengthened with CFRP sheets. Regarding the specimen series D-S-T (Fig. 4d), the CFRP strips covering the transition curvature part on the main

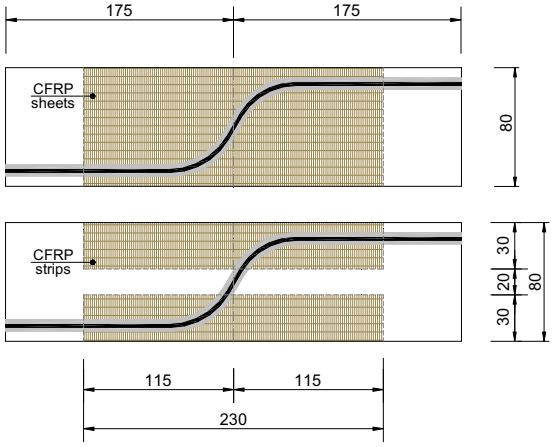

Fig. 1. Geometry of CFRP patch strengthened joints.

Table 2
Chemical compositions and mechanical properties of steel, carbon fibre and adhesive.

Type	Chemical composition (%)					Mechanical properties			
	C	S_i	M_n	P	S	Yield strength (MPa)	Elastic modulus (MPa)	Tensile strength (MPa)	Elongation (%)
Steel (Q345)	0.15	0.22	1.24	0.016	0.010	380	2.1×10^5	510	25
Carbon fibre (UT70–30)	–	–	–	–	–	–	2.52×10^5	4216	1.76
Adhesive (XH 180)	–	–	–	––	–	–	3.5×10^3	55	1.6

Fig. 2. Experimental test setup.

plate shift the crack initiation location to the vicinity of the inclined fold of the corrugated plate, thus resulting in a relatively longer crack propagation distance in the width direction.

3.2. Monotonic loading results

The comparison of the relationships between applied tensile stress and displacement is shown in Fig. 5. All the test specimens exhibit almost linear behaviour within the overall loading range. In this relation, the rigidity of the CFRP strengthened joint can be estimated from the slope of this linear relation. As expected, all reinforced joints exhibit greater rigidity with respect to the bare steel joints without strengthening. The increase of CFRP layers from one in the specimen series D-S-F to three in the specimen ser-ies D-T-F results in a significant increase of rigidity. The compari-son of the specimen series D-S-F and D-S-T shows that the rigidity of the welded joint strengthened with CFRP strips at the transition curvature is similar though slightly lower with respect to that with CFRP sheets on the double sides of the weld bead when the applied stress is greater than 80 MPa. The load induced dis-placement becomes obviously greater for the specimen series S-S-F with only one side strengthening than that for the specimen with double side reinforcement.

3.3. Fatigue life results

A graphical presentation of the test results in the relation of stress range and the number of cycles along with the fatigue detail categories of AASHTO LRFD [26] is shown in Fig. 6. For the sake of comparison, the former fatigue experiment data [24,25] of the welded joints with similar characteristic parameters are also plotted with counterpart mean and mean plus/minus two standard deviation lines. Visual inspection indicates that the scattered data of the bare steel joints of identical configuration lies between the Categories *B* and *B′*. Subsequent to the CFRP strengthening, the counterpart test data were mostly improved approaching or even above the Category *B*, and higher than the upper confidence interval (mean plus two standard deviations) of the test data of the bare steel joints.

Specimen series D-T-F with three CFRP layers reinforcement has gained longest life extension with an average increase of 91% with respect to the bare steel joints. Also, the improvement is obvious when comparing with that of the series D-S-F which gained approximately 58% enhancement. The life improvement with multiple CFRP layers can be expected as the extra force carried by the bonded layers above the first ones, although the distribution of the tensile load of the main plate is directly taken by the adhesive to first layer of CFRP.

Specimen series S-S-F with single-layered CFRP sheets only on the one side of the main plate has a life extension of approximately 15% greater compared to the specimen series D-S-F. However, the effect of extension is subjected to the variation as observed from the scatter of fatigue data. This is owing to the fact that the external strengthening only on the top side (containing welded details) of the main plate produces partial reinforcement effect and renders the bottom side (without welded details) carrying greater tensile stress than the top ones. This may reduce the tensile stress to some extent at the crack initialization location thus aiding the fatigue life extension.

Specimen series D-S-T is of particular interest as this series is identical to D-S-F with the exception that only the transition curvature is strengthened with the CFRP strips. The increase of fatigue life over the bare steel joints is effective for the specimen series D-S-T as compared to the series D-S-F, although the mutual average difference is within the range of 5%. This is in agreement with the aforementioned crack propagation mode observation in which the crack initiation location is somewhat shifted to the location near the end of the transition curvature and further away from the plate edge. The result of this comparison underscores the importance of the repair at the transition curvature location for the welded joints with corrugated plates. In other words, the proper strengthening effect can be achieved given that the repair at the welded details near the transition curvature between the longitudinal fold and the inclined fold is sufficient.

4. Numerical modelling

4.1. Analytical model description

The geometric representation of a half-unit of corrugated plate and its related welded details is schematically plotted in Fig. 7. The corrugation related parameters are θ_c for the inclined fold and θ_t for the transition curvature (centre angle). The rest of the parameters given for the corrugation and the main plate are the weld leg length (W_{fm}), the corrugated plate thickness (t_w), the depth of corrugation (h_c), the curvature radius (R_t), the length of the inclined fold (l_i) and the width of main plate (b_0). Assuming the curvature

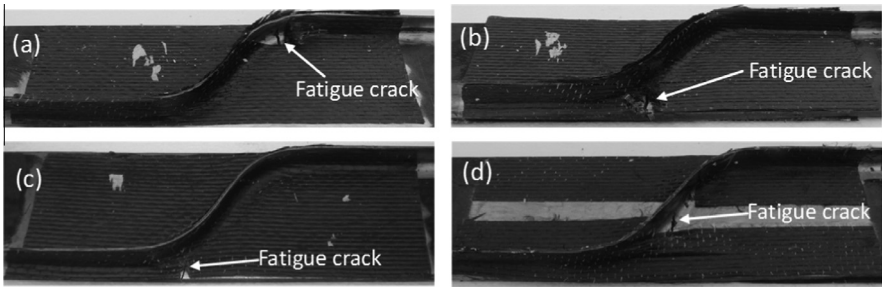

Fig. 3. Fatigue cracks at strengthened welded joints: (a) D-S-F, (b) D-T-F, (c) S-S-F, and (d) D-S-T.

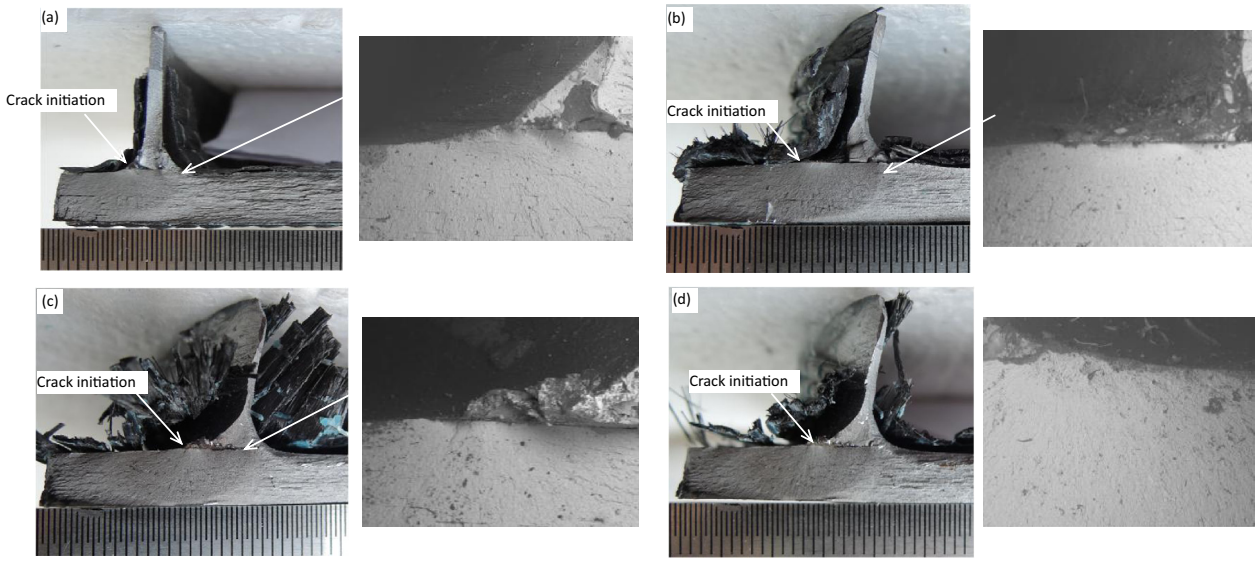

Fig. 4. Typical fatigue fracture surface of test specimens under 160 MPa: (a) D-S-F, (b) D-T-F, (c) S-S-F, and (d) D-S-T (the crack striation graph relating to the other half part opposite to the displayed fracture surface).

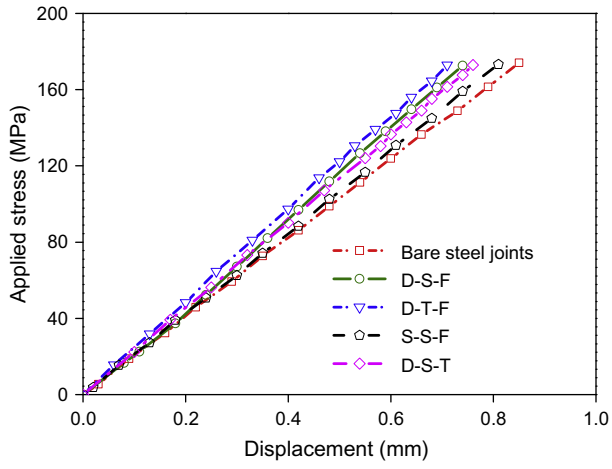

Fig. 5. Relationships between applied tensile stress and displacement of test specimens.

centre is located at the point of *O'* and its contour is in the form of a part of circular arc, the corresponding arc length is represented by $R_t\theta_t$. Based on the crack initiation observed in the fatigue test mentioned earlier, two critical sections, namely Sections 1.1 and 2.2, were chosen at the end of the inclined fold joining transition curvature, as shown in Fig. 7. Both sections are located at the internal and external sides of corrugation and in line with the direction of longitudinal stress. Since the fatigue crack propagates perpendicular to the tensile stress direction, the analytical model can be represented by a two dimensional analytical model allowing for the embedded crack at the weld toe. Through trigonometric substitution, the projected thickness of the corrugated plate (W_w), the weld leg lengths on the internal (W_i) & external (W_e) sides, and the distance between *O'* to the given sections along the transverse direction of the main plate in the direction of the *y*-axis can be deduced from R_t, W_{fw}, t_w, θ_t and θ_c, as listed in Table 3. Regarding the welded details on the Section 1.1, the slope angle, α_c, of the projected fillet weld outline is related to θ_c. Considering the weld leg lengths are bilaterally symmetrical with the corrugated plate, α_c can be given by:

$$\tan(\alpha_c) = \sin(\theta_c)\tan(\theta_f) = \frac{W_{fw}}{W_i} = \frac{W_{fw}}{W_e} \quad (1)$$

where θ_f is the weld flank angle on the fillet perpendicular to the weld toe line. If θ_f is assumed as a constant as 45°, the α_c can be rewritten in the form as:

$$\alpha_c = \text{atan}[\sin(\theta_c)] \quad (2)$$

It should be noted that the above equation becomes invalid for the Section 2.2, in which parts of arc curves rather than straight lines are involved in the weld toe line pattern. Thus, α_c can be deduced only from W_{fw}/W_i and W_{fw}/W_e ratios relating to the internal and external sides of the transition curvature respectively. With the aid of the equations outlined in Table 3, the relation

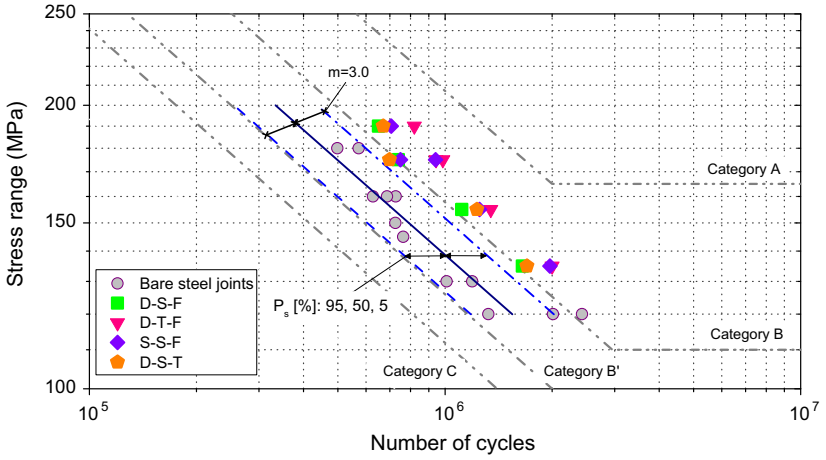

Fig. 6. Comparison of fatigue test results of strengthened welded joints & bare steel joints with *S–N* curves for AASHTO fatigue detail categories.

between α_c and θ_c for the Sections 1.1 and 2.2 can be further obtained and plotted in Fig. 8. It can be seen that α_c computed from the Section 1.1 is almost equal to that on the external side of Section 2.2. In the latter case, by contrast, the value of α_c estimated from the external side is greater than that from the internal side of the transition curvature when the value of θ_c is small. However, this difference is gradually reduced with the increase of θ_c and can be neglected as the value of θ_c is greater than 45°, which satisfies the symmetric condition about the mid-thickness of the corrugated plate.

Given aforementioned geometric details in the analytical model, the finite element analyses (FEA) were carried out using the ANSYS Academic Research, v.12.1 software package [28]. The FEA was used to determine the stress intensity factor (SIF) of mode I (K_I) which is directly relevant in evaluating the problem of a crack at the weld toe under tensile stress. As shown in Fig. 9(a), a half model was used to take advantage of symmetry. The model has regions covering the welded details and utilizes Plane 183 element. This element has 6 nodes or 8 nodes with two degrees of freedom at each node and is well suited in modelling irregular meshes. Two

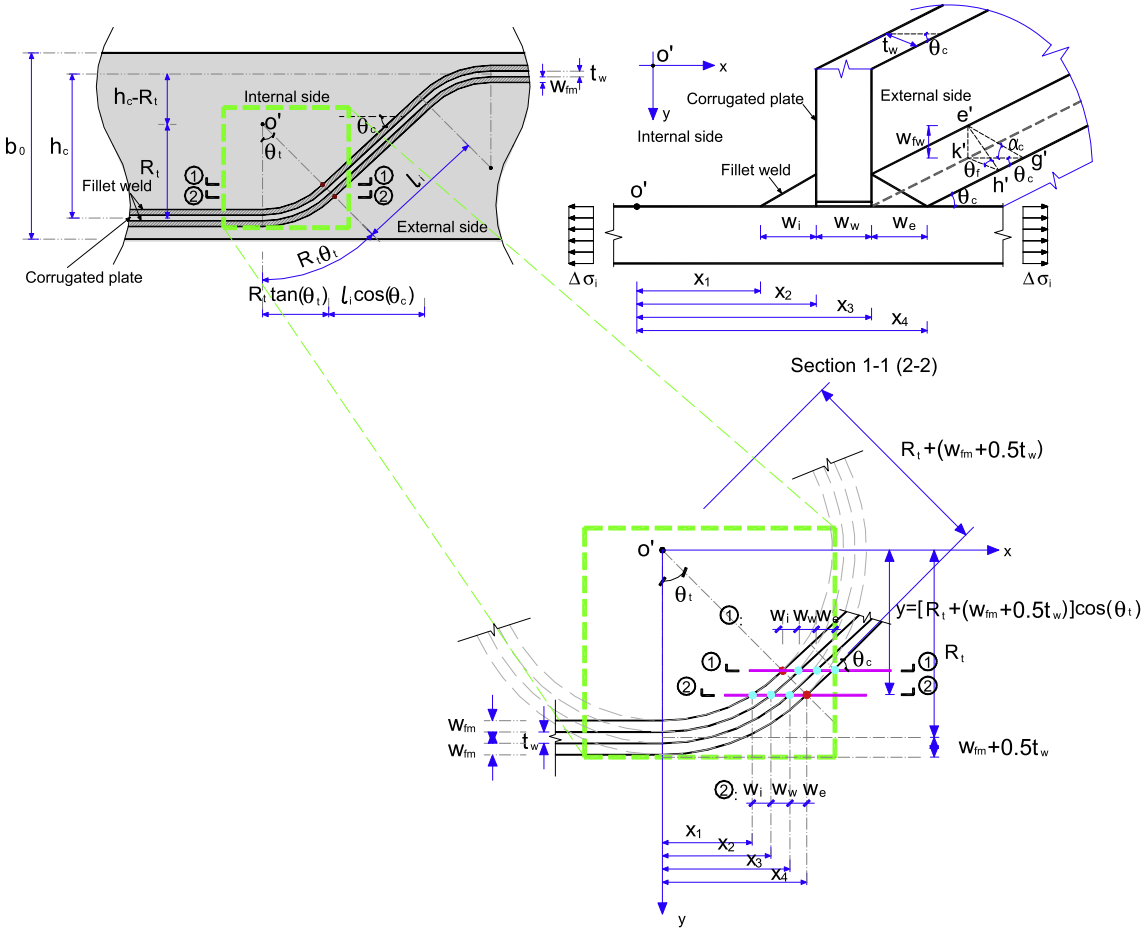

Fig. 7. Geometric relation of analytical welded details.

Table 3
Geometric parameters of joint details.

	y	W_i	W_w	W_e
Section 1.1	$[R_t - (W_{fw} + 0.5t_w)]\cos(\theta_t)$	$W_{fw}/\sin(\theta_c)$	$t_w/\sin(\theta_c)$	$W_{fw}/\sin(\theta_c)$
Section 2.2	$[R_t + (W_{fw} + 0.5t_w)]\cos(\theta_t)$	$x_2 - x_1$	$x_3 - x_2$	$x_4 - x_3$
$x_1 = \{[R_t - (W_{fw} + 0.5t_w)]^2 - [R_t+(W_{fw} + 0.5t_w)]^2\cos^2(\theta_t)\}^{0.5}$,				
$x_2 = \{(R_t - 0.5t_w)^2 - [R_t+(W_{fw} + 0.5t_w)]^2\cos^2(\theta_t)\}^{0.5}$				
$x_3 = \{(R_t + 0.5t_w)^2 - [R_t+(W_{fw} + 0.5t_w)]^2\cos^2(\theta_t)\}^{0.5}$, $x_4 = [R_t+(W_{fw} + 0.5t_w)]\sin(\theta_t)$				

Note: θ_f is taken as 45°, thus $e'k' = k'h'$, i.e. $W_{fw} = W_{fm}$, can be assumed.

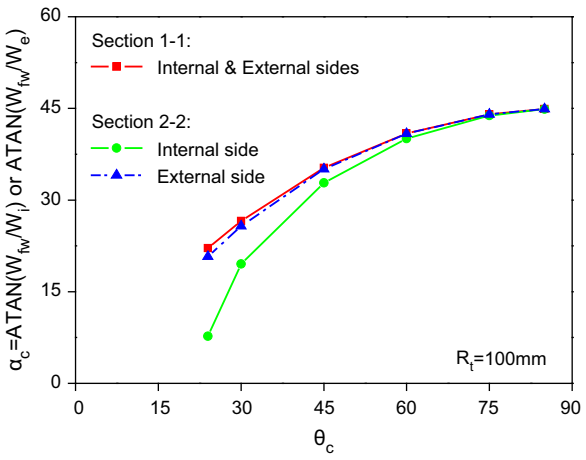

Fig. 8. Comparison of α_c and θ_c related to Sections 1.1 and 2.2.

flanks of the crack face were modelled and their related nodes were separate but coincident in nodal coordinates. The concen-trated mesh was used at the crack tip with mesh-size control-concentrated keypoint and quadratic singular elements. A typical mesh used in the finite element analysis is shown in Fig. 9(b). The material properties used in the modelling were as reported for the test specimens. Poisson's ratios for the steel, CFRP and adhesive were taken as 0.3, 0.35 and 0.28 respectively. The main plate, CFRP sheets and adhesives were bonded together using CONTA178 element which has two nodes with three degrees of freedom at each node. The load transfer was considered from the steel to the adhesive and then into the CFRP layer. A uniformly dis-tributed tensile load was applied at the one end of the main plate. A typical stress contour result of the finite element model is also shown in Fig. 9(b). The crack tip below the weld toe is seen to have significant plasticity. The value of K_I for various crack lengths was obtained using *J*-integral method from path integration around crack tip. For the purpose of validation, the FEA result was compared with a reported theoretical calculation [29] of the crack at the toe of bare fillet welds with the flank angles of 30° & 45°. The finite element model with $\alpha_c = 60°$ was also analyzed as an addition. The comparison results with the crack length (a) varying from 0.5 to 2.5 are shown in Fig. 10. It is apparent that the result of K_I predicted by the FEA compares well with that given by the the-oretical calculation especially for relatively large value of a. Also, K_I is amplified when the value of α_c is increased from 30° to 60°.

4.2. Parameter variation analysis

As indicated from the results presented in the previous section, the stress concentration at the weld toe is determined by the structural details of the fillet weld as well as the CFRP laminate. Meanwhile, the finite element model in this study can provide reliable

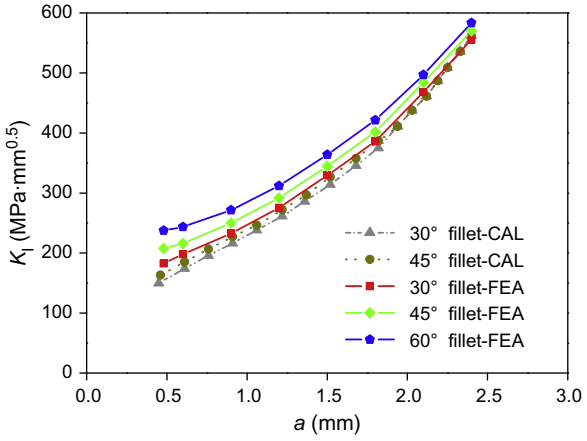

Fig. 10. Comparison of K_I obtained from theoretical calculation and FEA.

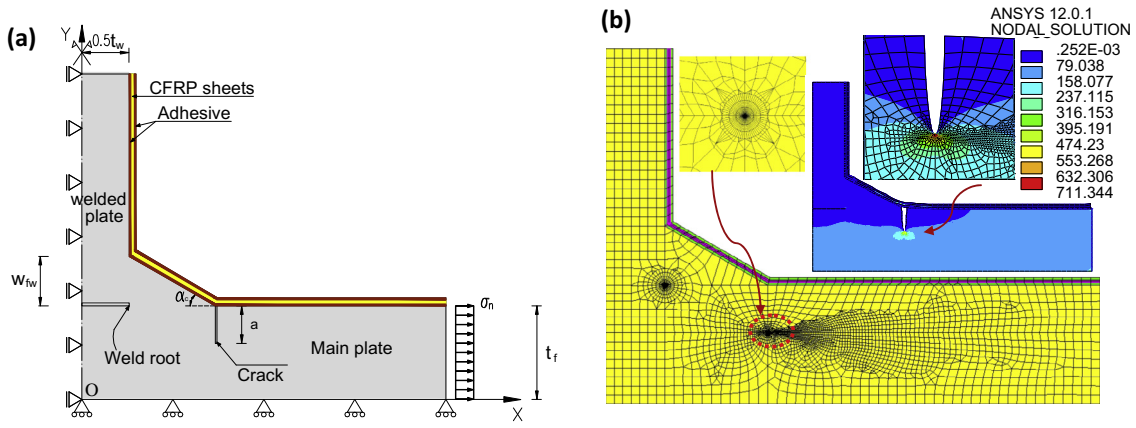

Fig. 9. Illustration of finite element analytical model: (a) Boundary condition, (b) mesh refinement and resultant stress contours.

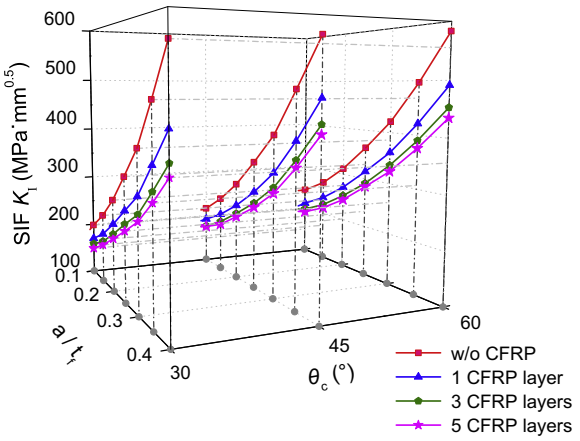

Fig. 11. Effect of the number of CFRP layers on K_I.

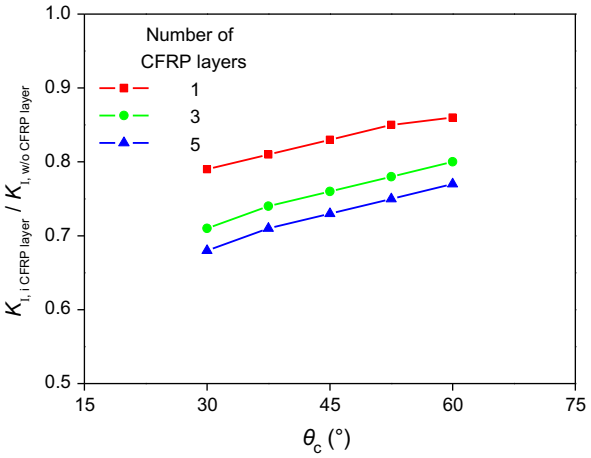

Fig. 12. Effect of the number of CFRP layers on $K_{I,\ i\ CFRP\ layers}/K_{I,\ w/o\ CFRP\ layer}$ ($a/t_f = 0.3$).

estimation of K_I related with a. To better understand related influences on the stress concentration of the CFRP strengthened welded joints, it is necessary to conduct a parametric study through numerical approach. In this part of study, the influencing parameters of the number of CFRP layers and the elastic modulus of carbon fibre (E_{CF}) & adhesive (E_{AD}) are investigated with the variation of θ_c (derived from α_c) and the ratio of (crack length) to t_f (the thickness of the main plate).

4.2.1. Effect of the number of CFRP layers

As mentioned earlier, the tensile stress is transferred from the steel to the adhesive and the CFRP layer when the CFRP strengthened welded joint is subjected to tensile loading. The number of the CFRP layers would in turn influence the fatigue strength of the strengthened welded joints. Regarding this, the number of strengthened CFRP layers varying from one to five and the corrugation angle varying from 30° to 60° was taken in this parametric study.

The effect of the number of CFRP layers on the value of K_I with the variation of θ_c and a/t_f is shown in Fig. 11. Generally, it can be observed that the CFRP strengthening significantly reduces K_I from the full range of the variation of a/t_f. It is noted that when single CFRP layer is used for strengthening, the increase of K_I for the specimens with θ_c varying from 30° to 60° is about 25% when $a/t_f = 0.1$; similarly, a slightly greater increase of 28% is observed for the case of the specimens with five CFRP layers. In contrast, this increment is reduced for the case of $a/t_f = 0.4$, which corresponds to 15% and 22% for the specimens with single and five CFRP layers. The effect of a/t_f on the value of K_I is significant from the observation that the single CFRP layered specimens with θ_c at 30° and 60° exhibit an increase of 111% and 77% when a/t_f is enhanced from 0.1 to 0.3. By further increasing the number of CFRP layers to five, the reduc-tion of the increment of K_I are 77% and 75% for the specimens with θ_c at 30° and 60° respectively. The comparison of the ratio between K_I of the specimens with different number of CFRP layers ($K_{I,i\ CFRP\ layer}$) and these with no CFRP strengthening ($K_{I,w/oCFRP\ layer}$) shows an increase trend with the increase of θ_c, as an example shown in Fig. 12. Thus, the reinforcement of using greater amount of CFRP layers is more effective for the specimens with relatively smaller corrugation angles and deeper cracks.

4.2.2. Effect of the modulus of carbon fibre

The effect of the modulus of carbon fibre on the stress intensity factor is presented in Fig. 13 with the influencing factors as the number of CFRP layers and a/t_f ratio. Taking into account the corrugated web related parameters, the analytical results of the specimens with $\theta_c = 30°$ and 60° are also compared.

It can be observed that an increase in the carbon fibre modulus from 1×10^5 MPa to 5×10^5 MPa to some extent reduces the value of K_I. The amount of this reduction is also influenced by θ_c. For the specimens with $\theta_c = 30°$, the reduction ratio of K_I decreases from 0.93 to 0.89 for the case of $a/t_f = 0.1$ and from 0.88 to 0.85 for the case of $a/t_f = 0.4$. By contrast, such reduction becomes insignificant for the specimens with $\theta_c = 60°$, i.e. the reduction ratio of K_I decreases from 0.97 to 0.94 for the case of $a/t_f = 0.1$ and from 0.95 to 0.93 for the case of $a/t_f = 0.4$. To further the understanding,

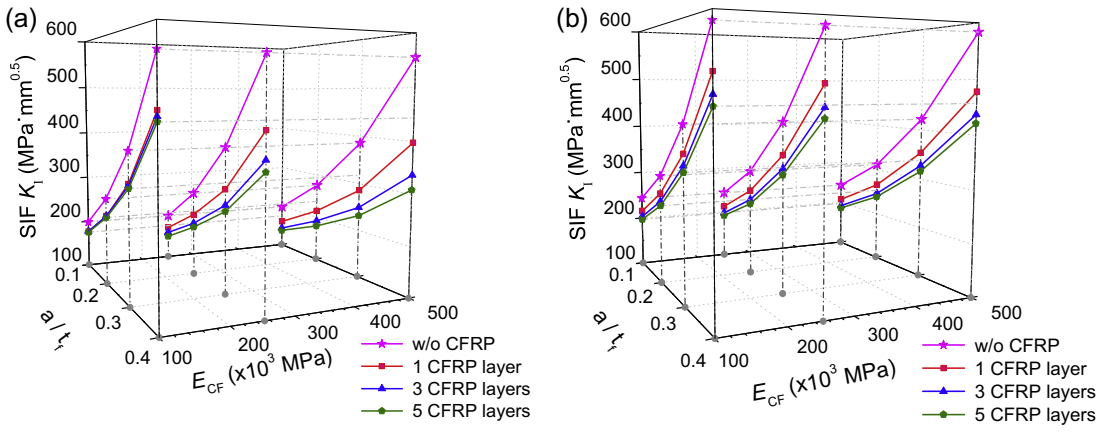

Fig. 13. Effect of carbon fibre modulus on K_I: (a) $\theta_c = 30°$, (b) $\theta_c = 60°$.

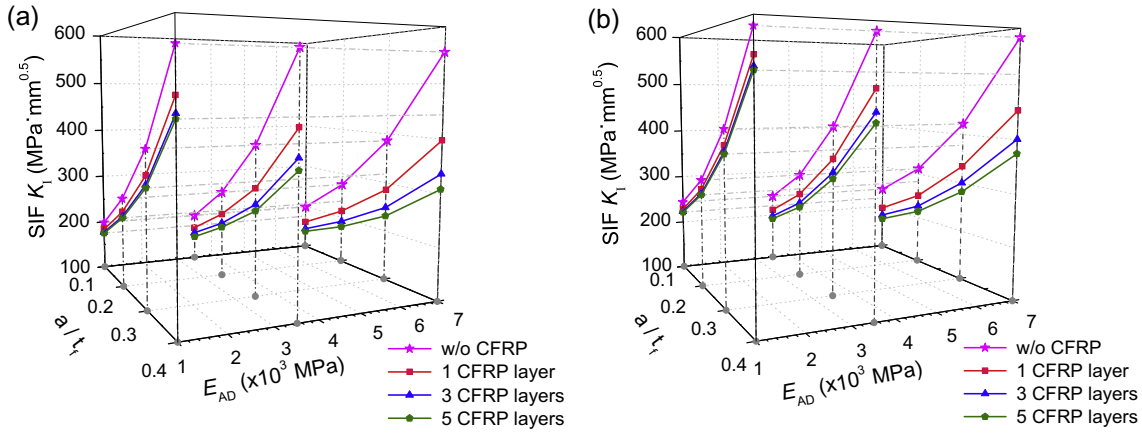

Fig. 14. Effect of adhesive modulus on K_I: (a) $\theta_c = 30°$, (b) $\theta_c = 60°$.

aforementioned $K_{I,i\ CFRP\ layer}/K_{I,w/o\ CFRP\ layer}$ ratio was also chosen for comparing the specimens when $a/t_f = 0.3$. As plotted in Fig. 15, the general trend of the curves regarding the reduction of $K_{I,i\ CFRP\ layer}/K_{I,\ w/o\ CFRP\ layer}$ with the increase of the number of CFRP layers is almost not influenced by the enhancement of the modulus of carbon fibre as well as θ_c. However, the gap between the curves corresponding to different carbon fibre modulus values is reduced with the increase of the θ_c. This also indicates the influence of the carbon fibre modulus on the K_I becomes insignificant with the increase of θ_c.

4.2.3. Effect of the modulus of adhesive

The laminating adhesive in the specimens is supposed to transfer the stress from the main plate. The modulus of adhesive also influences the failure mode of the strengthened joints. To compare this effect, the adhesive modulus, with its value of 1000 MPa, 3500 MPa and 7000 MPa, was taken as a varying parameter in the study.

As shown in Fig. 14, the value of K_I is significantly reduced with the increase of the modulus of adhesive. Also, it can be seen that the increase of E_{AD} from 1000 to 7000 results in a related reduction of 15% and 19% when a/t_f is increased from 0.1 to 0.4 for the specimens with $\theta_c = 30°$ and single layered CFRP strengthening. In contrast, this reduction is enhanced to 28% and 37% for the specimens with identical value of θ_c and five layered CFRP strengthening. Thus, this observation indicates that the increase of adhesive modulus is more effective in the reduction of K_I especially for the specimens with greater number of CFRP layers.

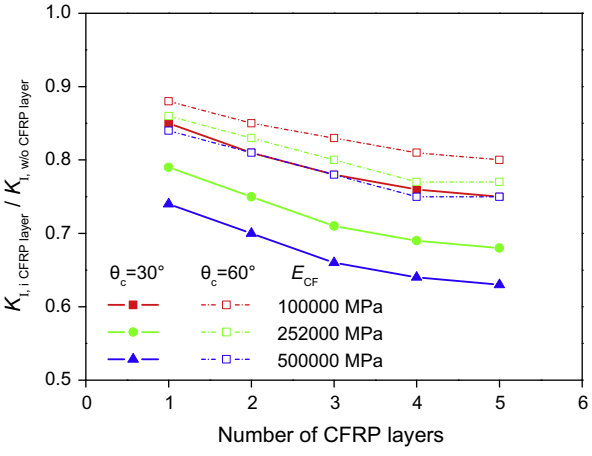

Fig. 15. Effect of carbon fibre modulus on $K_{I,\ i\ CFRP\ layers}/K_{I,\ w/o\ CFRP\ layer}$ ($a/t_f = 0.3$).

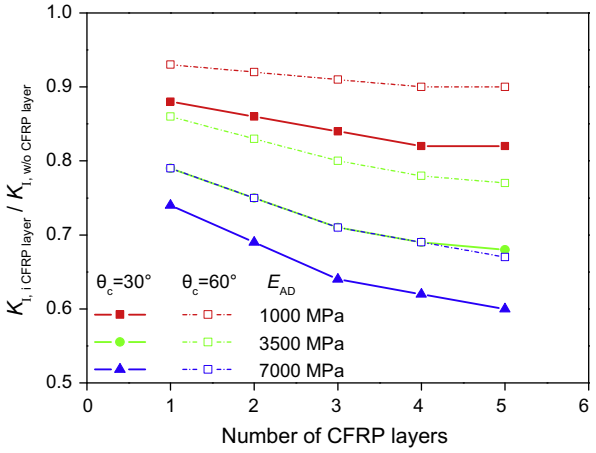

Fig. 16. Effect of adhesive modulus on $K_{I,\ i\ CFRP\ layers}/K_{I,\ w/o\ CFRP\ layer}$ ($a/t_f = 0.3$).

To compare the combined influence of θ_c in this study, the numerical results were also selected and displayed as the $K_{I,\ i\ CFRP\ layer}/K_{I,\ w/o\ CFRP\ layer}$ ratio for the case of $a/t_f = 0.3$, as shown in Fig. 16. Visual inspection shows that the general trend of the rela-tion between this reduction ratio and CFRP layer number is slightly influenced by the increase of E_{AD} and θ_c. By changing only the value of θ_c, it can be observed that the specimens with $\theta_c = 30°$ have greater reduction value of $K_{I,\ i\ CFRP\ layer}/K_{I,\ w/o\ CFRP\ layer}$ than those with $\theta_c = 60°$. Also, the increase of adhesive modulus seems to be effective in both cases in the reduction of the $K_{I,\ i\ CFRP\ layer}/K_{I,\ w/o\ CFRP\ layer}$ ratio.

5. Summary and conclusion

An experimental and numerical study was conducted to investigate the effectiveness of the use of CFRP sheets and strips in strengthening the welded joints with corrugated steel plates. Since the welded details in such joints are related with the corrugation pattern on the main plate, its stress concentration mode is different from that of common fillet welded joint and is not yet well understood. The experimental program was conceived to study the fatigue life improvement of such joints with CFRP strengthening methods, including the use of different number of CFRP layers and layout of CFRP sheets or strips, i.e. (a) repair on the one side of

the main plate containing welded details, and (b) repair only to the transition curvature location correspondingly on the both sides of the main plate. The test results indicate that the fatigue crack generally occurred in the region of the transition curvature between the longitudinal fold and the inclined fold of the corrugated plate. The three CFRP layered specimen and the transition curvature region only reinforced specimen performed well. It appeared from the fracture surface that the local crack initiation within the curvature was retarded to some extent and shifted from within the transition curvature to the vicinity of the inclined fold of the corrugation.

The rigidity of the welded joints was found to increase for the specimens with CFRP strengthening. The improvement is increased with the increase of the number of CFRP layers and reinforcement on the both sides of the main plate. The fatigue experimental results have demonstrated that the CFRP strengthening methods adopted in this study greatly enhance the fatigue life of the bare steel joints from the range between the Categories B and B' to that approaching or even above the Category B of AASHTO LRFD. Comparing the strengthening methods in this study, it is evident that the single CFRP layered specimens with one side reinforcement exhibit longer life than those with double side reinforcement which amount to 85% and 58% of average fatigue life improvement respectively with respect to the bare steel joints. Also, the transition curvature region only reinforced specimens showed a similar life improvement when compared with those with full width reinforcement on the double side. It therefore indicates the effectiveness of using the transition curvature region reinforcement and the single side reinforcement in prolonging the fatigue life of such welded details.

A simplified two dimensional analytical model taking into account the parameters of the corrugation angle and the critical section of fatigue crack initiation was implemented to examine the stress intensity factor of mode I (K_I). The proposed analytical model was studied using the finite element method. The analytical result shows that the developed numerical model achieved acceptable correlation with previously reported theoretical calculation. Afterwards, from a parametric study, the effects of three CFRP laminate related parameters, i.e. the number of CFRP layers and the moduli of carbon fibre & adhesive, on the stress intensity factor were investigated. It was concluded that the increase of CFRP layers has significant effect on the decrease of K_I for the specimens when the corrugation angle (θ_c) is relatively small and crack depth is relatively large. The higher modulus of carbon fibre produces greater reduction of K_I for the specimens with varying number of CFRP layers; notwithstanding that, such reduction is less significant for the specimens with larger value of θ_c. For the adhesive modulus, its enhancement in the specimens together with smaller value of θ_c has larger reduction of K_I with respect to the unreinforced specimens; however, the general trend of such decrease is not significantly affected by the change of θ_c. Although the model studied herein is limited in the welded joint details with the main plate subjected to tension, it can be regarded as a basis for the analysis of beam form structural details under combined loading condition.

Acknowledgements

The research presented was sponsored by the National Natural Science Foundation of PR China (Nos. 51308363 and 11327801) and the Scientific Research Foundation for the Returned Overseas Chinese Scholars (No. 2013-1792-9-4). The authors are grateful for the contributions of the students, X.K. Liu, H. Xue, and F. Hou, who have assisted in the preparation of test samples. The authors would also like to thank the College of Mechanical Engineering, Sichuan University of Science and Engineering, especially Mr L. Fu, Mr Y.Q. Zhang and Prof. G.Z. Hu, for their helps in coordinating the fatigue tests.

Reference

[1] Miki C. Bridge Engineering Learned from Failure fatigue and Fracture Control. Proceedings of Bridge Maintenance, Safety, Management and Cost Watanabe. Tokyo: Tokyo Institute of Technology; 2004.
[2] Miki C. Retrofitting Engineering for Steel Bridge Structures. IIW-XIII-WG5-74-7. International Institute of Welding; 2007.
[3] FHWA. Manual for repair and retrofit of fatigue cracks in steel bridges, Report, FHWA-IF-13-020, FHWA; 2013.
[4] Teng JG, Chen JF, Smith ST, Lam L. FRP strengthened RC structures. Chichester, England: John Willey and Sons. Ltd.; 2002.
[5] Moon DY, Zi G, Lee DH, Kim BM, Hwang YK. Fatigue behaviour of the foam-filled GFRP bridge deck. Composite Part B-Eng 2009;40(2):141–8.
[6] Meneghetti G, Quaresimin M, Ricotta M. Damage mechanisms in composite bonded joints under fatigue loading. Composite Part B-Eng 2012;43(2):210–20.
[7] Madhoushi M, Ansell MP. Behaviour of timber connections using glued-in GFRP rods under fatigue loading. Part I: in-line beam to beam connections. Composite Part B-Eng 2008;39(2):243–8.
[8] Wu Z, Wang X, Iwashita K, Sasaki T, Hamaguchi Y. Tensile fatigue behaviour of FRP and hybrid FRP sheets. Composite Part B-Eng 2010;41(5):396–402.
[9] Hollaway LC, Cadei J. Progress in the technique of upgrading metallic structures with advanced polymer composites. Prog Struct Eng Mater 2002;4(2):131–48.
[10] Deng J, Lee MMK. Fatigue performance of metallic beam strengthened with a bonded CFRP plate. Compos Struct 2007;78:222–31.
[11] Zhao XL, Zhang L. State-of-the-art review on FRP strengthened steel structures. Eng Struct 2007;29:1808–23.
[12] Mosallam, AS, Chakrabarti PR, Spencer E. Experimental investigation on the use of advanced composites & high-strength adhesives in repair of steel structures. In: 43rd International SAMPE Symposium May 31–June 4; 1998. p. 1826–37.
[13] Bassetti A, Nussbaumer A, Hirt MA. Crack repair and fatigue extension of riveted bridge members using composite materials. In: Bridge engineering conference, ESE-IABSE-FIB; 2000, p. 227–38.
[14] Miller TC, Chajes MJ, Mertz DR, Hastings JN. Strengthening of a steel bridge girder using CFRP plates. J Bridge Eng, ASCE 2001;6(6):514–22.
[15] Mertz DR, Gillespie Jr. JW, Chajes MJ, Sabol SA. Rehabilitation of steel bridge girders through the application of advanced composite materials. Final Report for NCHRP-IDEA Project 51. Washington, D.C.: Transportation Research Board; 2002.
[16] Tavakkolizadeh M, Saadatmanesh H. Fatigue strength of steel girders strengthened with carbon fiber reinforced polymer patch. J Struct Eng, ASCE 2003;129(2):186–96.
[17] Inaba N, Tomita Y, Shito K, Suzuki H, Okamoto Y. Fundamental study on a fatigue strength of a cruci-form welded joint patched a glass fiber reinforced plastic. Doboku Gakukai Ronbunshuu, JSCE 2005;VI-68(798):89–99. in Japanese.
[18] Nakamura H, Jiang W, Suzuki H, Maeda, Irube T. Experimental study on repair of fatigue cracks at welded web gusset joint using CFRP strips. Thin-Walled Struct 2009;47:1059–68.
[19] Chen T, Yu QQ, Gu XL, Zhao XL. Study on fatigue behavior of strengthened nonload-carrying cruciform welded joints using carbon fiber sheets. Int J Struct Stability Dyn 2012;12(1):179–94.
[20] Chen T, Yu QQ, Gu XL, Nie GH. Stress intensity factors (KI) of cracked non-loadcarrying cruciform welded joints repaired with CFRP materials. Composite Part B-Eng 2013;45(1):1629–35.
[21] Virlogeux M. Les Ponts Mixtes Associant l'Acier et le Beton Precontraint. Bulletin Ponts Metalliques 1992;15:25–68 (in French).
[22] JSCE. Design manual for PC bridges with corrugated steel webs. Research committee for hybrid structures with corrugated steel webs, Japan Society of Civil Engineers, Japan; 1998.
[23] Sause R, Abbas HH, Driver RG, Anami K, Fisher JW. Fatigue life of girders with trapezoidal corrugated webs. J Struct Eng, ASCE 2006;132(7):1070–8.
[24] Wang ZY, Tan LF, Wang QY. Fatigue strength evaluation of welded structural details in corrugated steel web girders. Int J Steel Struct 2013;13:707–21.
[25] Wang ZY, Wang QY. Fatigue assessment of welds joining corrugated steel webs to flange plates. Eng Struct 2014;73:1–12.
[26] AASHTO. AASHTO LRFD bridge design specifications. In: 3rd Ed, AASHTO, Washington, D.C.; 2005.
[27] GB/T1591-2008. High strength low alloy structural steels. Beijing: Standards Press of China; (2008) (in Chinese).
[28] ANSYS@Academic Research, Release 12.1, Help System, Structural Analysis Guide, ANSYS Inc.; 2009.
[29] Maddox SJ. An analysis of fatigue cracks in fillet welded joints. Int J Fract 1975;11(2):221–43.